



*Dedicated to Professor Zeno Simon
on the occasion of his 80th anniversary*

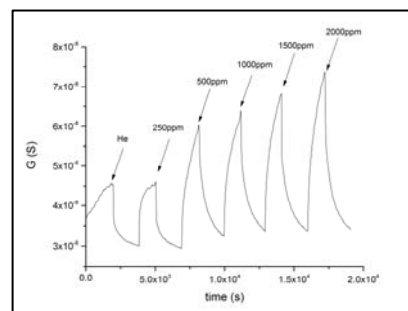
CARBON MONOXIDE SENSING PROPERTIES OF TiO₂

Paul CHESLER, Cristian HORNOIU,* Veronica BRATAN, Cornel MUNTEANU,
Mariuca GARTNER and Nicolae I. IONESCU

“Ilie Murgulescu” Institute of Physical Chemistry of the Roumanian Academy, 202 Splaiul Independentei, Bucharest, Roumania

Received June 16, 2014

The TiO₂ electrical conductivity was used to detect CO in gas atmospheres in absence of oxygen. The obtained results are discussed.



INTRODUCTION

Carbon monoxide (CO) is a highly toxic, colorless and odorless gas, making it undetectable to humans. This gas is the main product of incomplete oxidation of organic materials such as petroleum, oil or hydrocarbons. Carbon monoxide concentrations are particularly high in industries in which fossil fuels are burned in order to produce energy and in cities where there is a high traffic.¹⁻⁵ That is why CO needs special sensors and also warning systems to be detected.

The interaction of gases with transition metal oxides surfaces continues to be an active area of research.⁶⁻¹¹ The commercial sensors for CO, which usually contain semiconductor oxides, are based on changes in electrical conductivity due to oxygen chemisorption from the environment and to CO oxidation to CO₂.¹²

Redox chemistry on oxide surfaces is responsible for processes involving the selective oxidation of various organic molecules.^{6, 7, 13}

Measurements of the electrical resistance of metal oxides is used for the detection of gases such as CO, H₂ or hydrocarbons and it is due to the chemical reaction of these gases with oxygen adsorbed on the surface.^{9, 10}

The goal of this paper is to determine the variation of the electrical resistance of TiO₂ (powder) depending on the composition of the gas atmosphere in order to detect traces of CO in absence of oxygen, and also to establish a gas sensing mechanism.

EXPERIMENTAL

A commercial TiO₂ (anatase) powder (Rhone-Poulenc) was used.

* Corresponding author: chornoiu@icf.ro

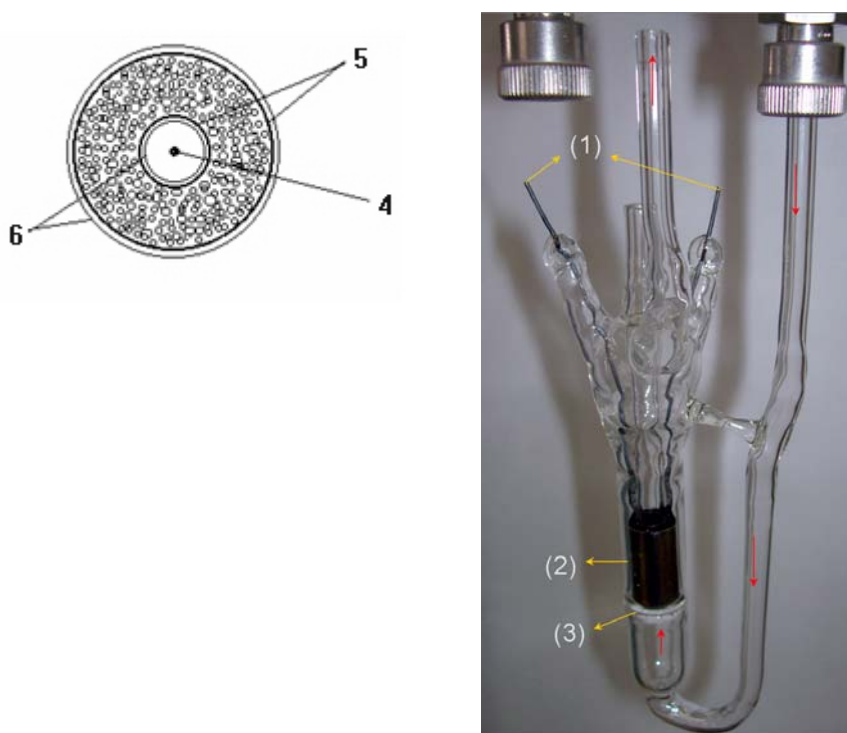


Fig. 1 – The reaction cell with: (1) Tungsten wires, (2) Coaxial tantalum electrodes (cylinder type), (3) Ceramic frit, (4) Thermocouple (slice view), (5) Coaxial tantalum electrodes (slice view), (6) Glass walls (slice view).

The XRD analysis was performed on a Rigaku Ultima IV apparatus, with $\text{CuK}\alpha$ $\lambda = 1.5406 \text{ \AA}$ radiation, in the $2\theta = 20\text{--}70^\circ$ range.

The morphology of the samples was investigated by scanning electron microscopy (SEM) using a high-resolution microscope, FEI Quanta 3D FEG model, at an accelerating voltage of 15 kV, in high vacuum mode with Everhart–Thornley secondary electron (SE) detector. Samples preparation was minimal and consisted in immobilizing the material on a double-sided carbon tape, without coating.

The electrical resistance R was measured on powder samples (having a volume of 1.5 cm^3 , and a size-fraction between $0.25\text{--}0.5 \text{ mm}$) under the influence of the gas/temperature, using a special reaction cell.¹⁴ This cell consists of two coaxial tantalum cylinders as electrodes, embedded in a Pyrex glass tube and connected by tungsten wires to a precision RLC bridge (HIOKI 3522-50), which was set at a fixed frequency of 1592 Hz. The sample is filling the annular space between the electrodes and is supported on a frit (see Fig. 1). Temperature in the powder bed was monitored with a thermocouple located in the center of the cell. In order to clean the powder sample of water traces and other contaminants, an initial heating was made in helium atmosphere, between room temperature and 400°C (with a ramp of $5^\circ/\text{min}$).

Electrical measurements were performed at different temperatures, from 200 to 450°C , with various concentrations of CO ($0\text{--}2000 \text{ ppm}$), obtaining the values of R when the solid-gas system has attained its equilibrium.

The samples were placed in a controlled atmosphere in a continuous flow of CO in He, with a flow rate of 72 mL /

min .¹⁵ Gas flows were provided by a calibrated system of mass-flow controllers (MFC). In order to simulate a fuel cell, oxygen gas is not present in the reaction chamber.

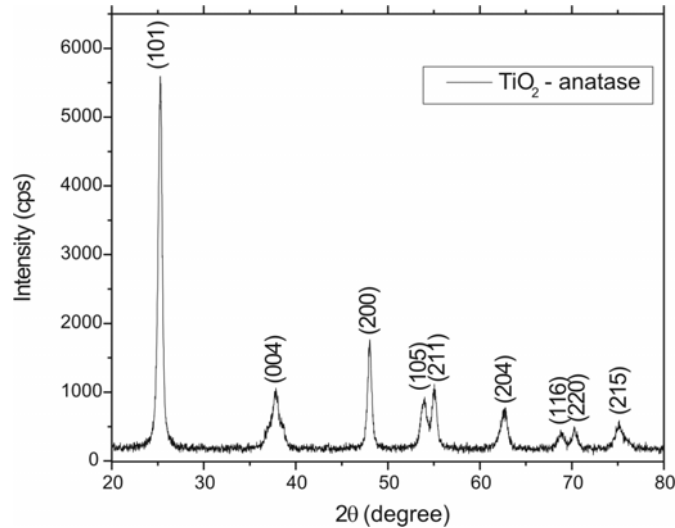
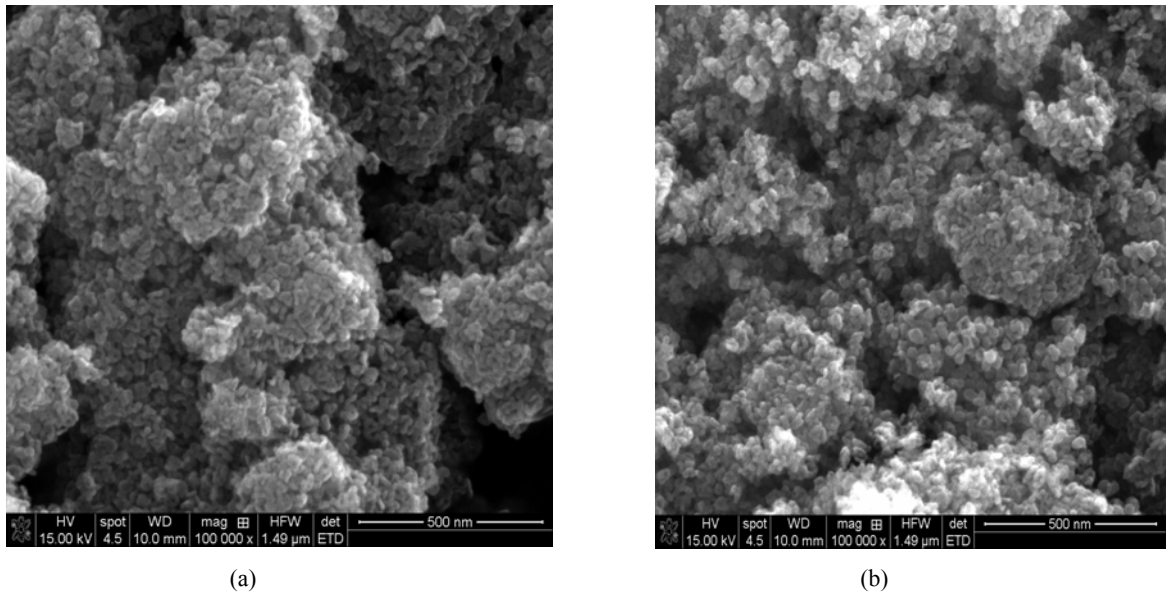
RESULTS AND DISCUSSION

Sample characterisation

The purity of the TiO_2 sample has been identified from the XRD pattern in Fig. 2. The sample has a crystalline structure, the peaks located at $25.27, 37.78, 48.02, 53.85, 55.01, 62.70, 68.79, 70.23, 75.03$ are assigned to (101), (004), (200), (105), (211), (213), (116), (220), (215) planes of the pure anatase phase, according to card number JCPDS 21-1272.

TiO_2 remains in its anatase structure during the reaction; crystallographic changes were not observed between the fresh and the tested samples.

From SEM images, any difference in the crystallographic structure of TiO_2 sample before and after reaction with CO at different temperatures was not noticed. The individual particles are nano-sized, with the tendency to agglomerate, forming clusters. All the samples can be re-used after testing with CO.

Fig. 2 – XRD spectrum of TiO₂ sample.Fig. 3 – SEM images of TiO₂ powder (a) before and (b) after testing with CO.

Sensor measurements

According to Caldararu *et al.* polycrystalline oxides (powders) may be modeled by a network consisting of highly conducting grains separated by poorly conducting inter-grain contacts.¹⁶

In our experimental conditions *i.e.* non-sintered, non-pressed powder, at a fixed and low frequency of 1592 Hz, the measured effective resistance (conductance) is dominated by Schottky-type barriers developed in inter-grain areas,⁹ thus the surface of the sample plays the major role in the electrical conductivity, while the bulk contribution could be considered negligible.

For an easier representation of the obtained results the sensitivity of the material (S) for CO,

was defined as the ratio between the electrical resistance of the sample in He (R_{He}) and the electrical resistance of the sample in CO (R_{CO}):¹⁷

$$S = \frac{R_{He}}{R_{CO}} \quad (1)$$

From Fig. 4 it can be observed that the sensitivity of TiO₂ sample increases strongly with the temperature, having a maximum at 400°C, temperature which will be considered the optimum work temperature of the material. For this optimum temperature, sample sensitivity is proportional to the concentration of CO. Also the sensitivity of the material increases with the increasing of CO concentration.

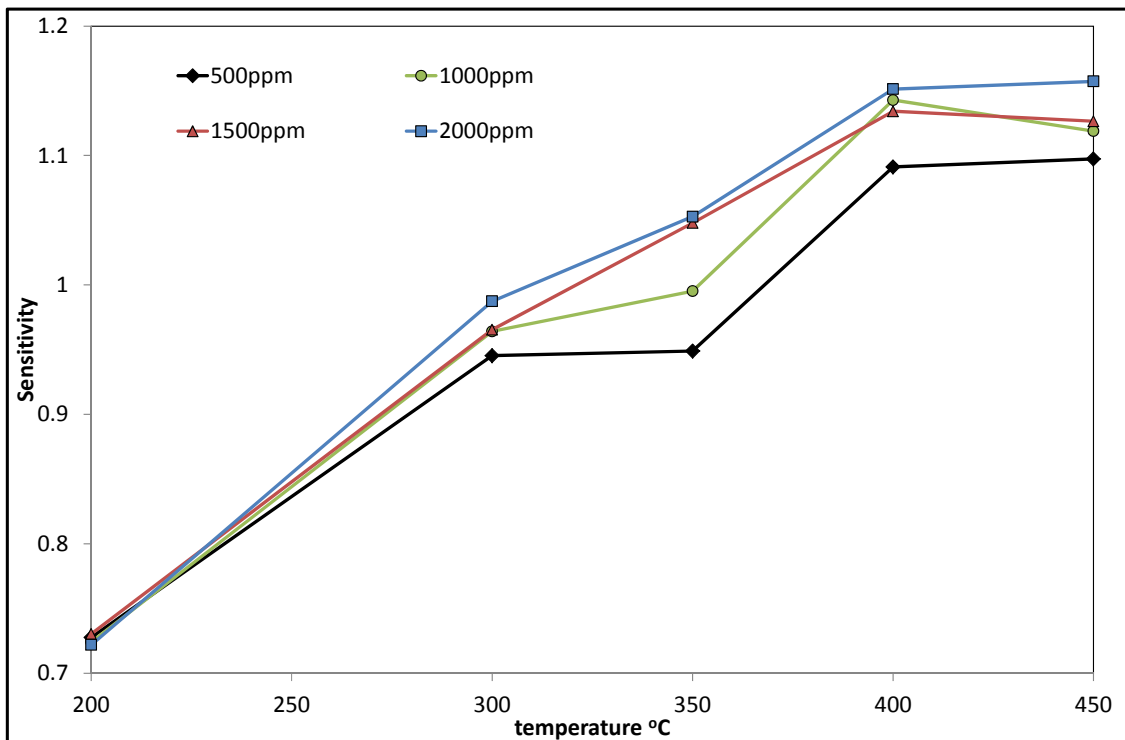


Fig. 4 – Electrical response of TiO₂ powder for various concentrations of CO depending on temperature.

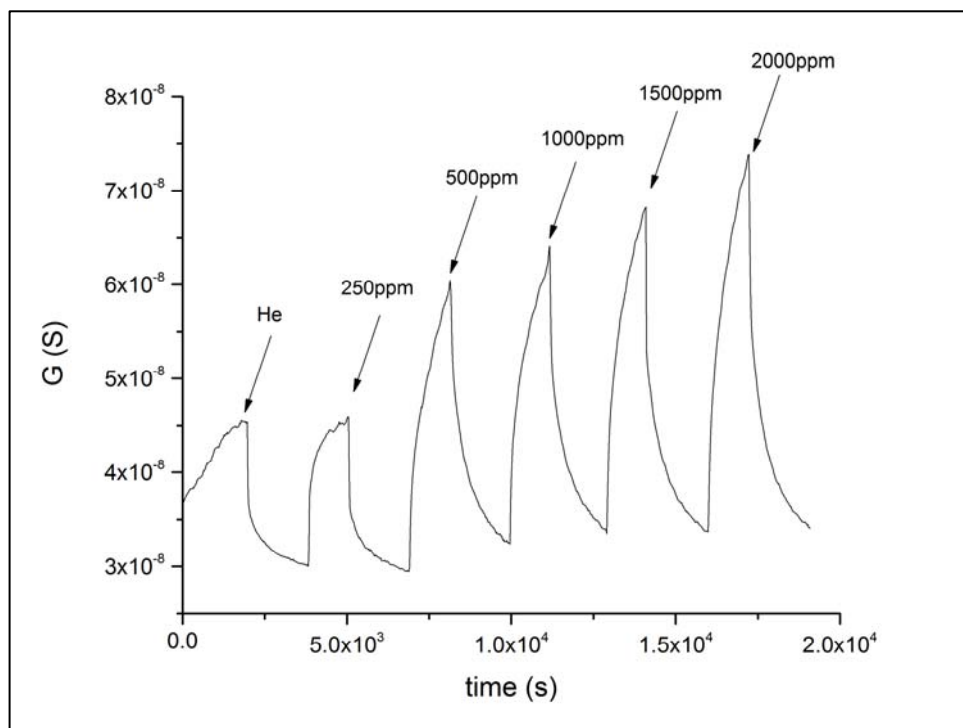


Fig. 5 – Electric response of TiO₂ sample at 400°C, for different CO concentration.

Considering the results from Fig. 4, the composition of the gaseous atmosphere (CO in an atmosphere of helium, without oxygen), the optimum work temperature and literature data,¹⁸ a reaction mechanism which involves the direct

reduction of Ti⁴⁺ on anatase surface could be proposed.

This reaction mechanism involves two stages: a first stage that takes place at low temperature (below 300°C), in which there is a physical

adsorption of CO on the surface of TiO₂ and a second stage that takes place at a higher temperature (over 300°C) in which catalytic oxidation of CO to CO₂ occurs, using lattice oxygen from TiO₂.

In the second stage, after desorption of CO₂, the reduced Ti²⁺ ions obtained are distributed through the lattice, resulting in a decrease of electrical resistance due to the electrons released in the reaction. Oxygen from the bulk of TiO₂ can re-oxidize these centers, resulting in surface regeneration of the sample.

In Fig.5 a full measurement cycle of TiO₂ sample over the entire range of CO concentrations at 400°C is presented. The sample conductance (G) increases when the injection of CO in the reaction cell begins, due to TiO₂ reduction process, electrons being released. When the CO flow is stopped, the conductance decreases, and the sensor enters the recovering stage. It can be seen that for a given concentration and a complete cycle of 3000 seconds (that includes an injection of CO for 1200 seconds, followed by achieving the stationary state in another 1800 seconds, with the CO flow stopped) the sensor recovery is complete, its conductance values returning to baseline.

The electrical resistance of a sensor can be correlated with partial pressure of the flowing gas¹⁹ using the equation:

$$R = ap^n \quad (2)$$

$$\text{or: } \ln R = \ln a + n \ln p \quad (3)$$

where a and n are constants.

Using the peak values of the conductance from Fig. 5 the electrical resistance values can be represented as a function of the partial pressure of the CO and plotted in Fig. 6.

The proposed CO to CO₂ oxidation mechanism is:



where V_o^+ is a charged oxygen vacancy and e^- the conduction electron.

The equilibrium constant K has the formula:

$$K = \frac{[TiO]_s p_{CO_2} [e^-]^2 [V_o^+]^2}{[TiO_2]_s p_{CO}} \quad (4)$$

where $[TiO]_s$ and $[TiO_2]_s$ are surface concentrations, according to the proposed model.

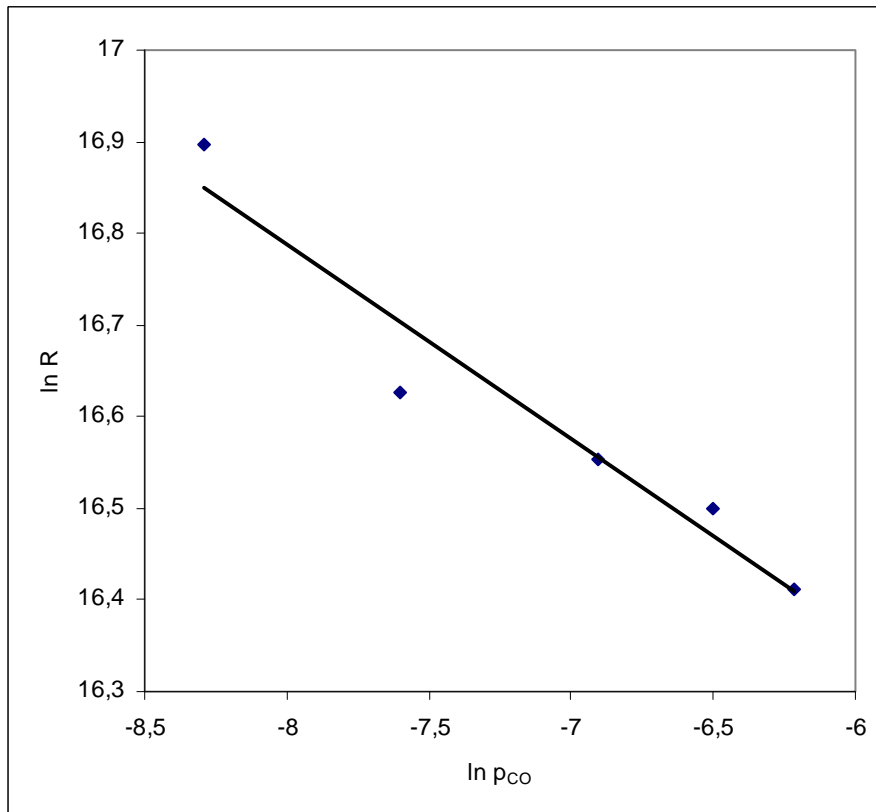


Fig. 6 – Arrhenius plot of electrical resistance as a function of partial pressure of CO.

The condition of electroneutrality requires that:

$$[e^-] = [V_o^+] \quad (5)$$

In this case, using relationship (4) one obtains:

$$K[TiO_2]_s p_{CO} = [TiO]_s p_{CO_2} [e^-]^4 \quad (6)$$

and finally,

$$p_{CO}^{1/4} = \alpha [e^-] \quad (7)$$

approximating that α , the ratio between the concentration of TiO and TiO₂ is a constant.

The concentration of electrons released in the reaction is proportional to the conductivity of the material:

$$\sigma \propto [e^-] \quad (8)$$

In this case:

$$\sigma \propto p_{CO}^{1/4} \quad (9)$$

Because:

$$R \approx \frac{1}{\sigma} \quad (10)$$

it results that :

$$R \propto \frac{1}{p_{CO}^{1/4}} \quad (11)$$

$$\text{or } R \propto p_{CO}^{-1/4} \quad (12)$$

From equation (12), it can be seen that the electrical resistance of the sample depend on the partial pressure of CO.

Correllating fig. 6 with equation (3) one identifies the slope $n = -0.2122$, close to $-1/4$. This value is in an agreement with the values of CO partial pressure obtained from relationship (12). This fact proves a good correlation between experimental data and the proposed mechanism for the oxidation of CO to CO₂.

CONCLUSIONS

Changes in electrical resistance of the TiO₂ sample due to CO oxidation on the surface were used to detect the presence of CO in the absence of oxygen. The electrical resistance of the samples depends on the partial pressure of CO in various ppm concentrations.

The TiO₂ (anatase) can be proposed for the development of a CO sensor in the absence of oxygen, for applications such as fuel cells, having a good performance in terms of gas sensitivity, operating temperature, stability and sensor recovery.

Acknowledgements: Support of the EU (ERDF) and Roumanian Government that allowed for acquisition of the research infrastructure under POS-CCE O 2.2.1 project INFRANANOCHEM - Nr. 19/01.03.2009, is gratefully acknowledged.

REFERENCES

1. C. Cobb and C.R. Cetzel, *J. Am. Med. Assoc.*, **1991**, 266, 659.
2. C.T. Meredith, *Brit. Med. J.*, **1988**, 296, 110.
3. C.C. Runyan, C. Johnson, J.Yang, A. Waller, D. Perkis and S. Marshall, *Am. J. Prev. Med.*, **2005**, 28, 102.
4. J. Varon, P.E. Marik, R.E. Fromm Jr. and A. Gueler, *J. Emer. Med.*, **1999**, 17, 87.
5. Recommendations for Occupational Safety and Health: Compendium of Policy Documents and Statements; U.S. Department of Health and Human Services, Public Health Service, Centers for Disease Control, National Institute for Occupational Safety and Health, DHHS (NIOSH): Cincinnati, OH, USA, 1992; Publication No. 92-100.
6. G. Centi and M. Misono, "Catalysis Today" vol. 41, Elsevier: Amsterdam, 1988, p. 1.
7. S. Poulston, N.J. Price, C. Weeks, M.D. Allen, P. Parlett, M. Steinberg and M. Bowker, *J. Catal.*, **1998**, 178, 658.
8. G. Mitran, A. Urdă, I. Săndulescu and I.C. Marcu, *React. Kinet. Mech. Catal.*, **2010**, 99, 135.
9. J.F. McAleer, P.T. Moseley, J.O.W. Norris and D.E. Williams, *J. Chem. Soc., Faraday Trans.*, **1987**, 83, 1323.
10. A. Vancu, R. Ionescu and N. Barsan, "Chemoresistive Gas Sensors. In Thin Film Sensors"; R. Ciureanu and S. Middelhoek (Eds.), Institute of Physics Publishing: Philadelphia, 1992.
11. M.J. Madou and S.R. Morrison, "Chemical Sensing with Solid State Devices", Academic Press, San Diego, CA, 1989.
12. C.T. Holt, A.M. Azad, S.L. Swartz, R.R. Rao and P.K. Dutta, *Sens. Actuators B*, **2002**, 87, 414.
13. L.M. Madeira, J.M. Herrmann, J. Disdier, M.F. Portela and F.G. Freire, *Appl. Catal. A*, **2002**, 235, 1.
14. M. Caldararu, D. Sprinceana, V.T. Popa and N.I. Ionescu, *Sens. Actuators B.*, **1996**, 30, 35.
15. V. Bratan, C. Hornoiu and N. I. Ionescu, *Rev. Roum. Chim.*, **2012**, 57, 513.
16. M. Caldararu, M. Scurtu, C. Hornoiu, C. Munteanu, T. Blasco and J.M. Lopez Nieto, *Catalysis Today*, **2010**, 155, 311.
17. C. Wang, L. Yin, L. Zhang, D. Xiang and R. Gao, *Sensors*, **2010**, 10, 2088.
18. P.K. Dutta, A. Ginwalla, B. Hogg, B.R. Patton, Z. Liang, P. Gouma, M. Mills, and S. Akbar, *J. Phys. Chem. B*, **1999**, 103, 4412.
19. N. Yamazoe and K. Shimanoe, *Sens. Actuators B*, **2008**, 128, 566.

